Bioscene

Bioscene
Volume- 22 Number- 03
ISSN: 1539-2422 (P) 2055-1583 (O)
www.explorebioscene.com

Optimization and Characterization of Copper Oxide Nanoparticles of *Cassia Angustifolia* Leaf Extract Prepared by Green Synthesis

[1]Anil Kumar Jangid, [2]Dr. Shikha Sharma

[1,2] Department of pharmaceutical Science, Lords University, Alwar, Rajasthan, India

Corresponding Author: **Anil Kumar Jangid**

Abstract: The present article discusses the effectiveness of the green synthesis method in the synthesis of copper oxide nanoparticles (CuO NPs) using Cassia angustifolia leaves. They enabled the investigation of the interactions of variables by the use of the response surface methodology and the Box-Behnken design. Characterization was carried out by UV-Vis, DRS, FTIR, XRD, SEM, TEM, and EDAX. The UV-Vis had a blue-shifted absorption peak at -400 nm. According to TEM and SEM, CuO NPs had a diameter of 20-62.5 nm and were round-shaped. The zeta potential was -22.6 mV, the average hydrodynamic diameter was 111.65 nm, and it implies that the nanoparticles were well stabilized. EDX detected only the existence of copper elements. Optimal synthesis occurred at 60°C and 7932 rpm. As it is indicated by the findings, the stable and crystalline CuO NPs have been green-synthesized, which can offer safer and more sustainable alteration of the conventional process.

Keywords: green synthesis; cassia angustifolia; nano-particles; copper-oxide; FTIR; TEM

1. Introduction

Nanotechnology stands at the cutting edge of modern innovation a dynamic, interdisciplinary domain where chemistry, physics, biology, and engineering converge to redefine the limits of material science [1,2]. By mastering the art of manipulating matter at the atomic and molecular scale (1–100 nm), researchers unlock extraordinary properties unseen in bulk materials, paving the way for breakthroughs once confined to the realm of science fiction [3,4].

This rapidly evolving field is not just about shrinking materials; it's about reimagining them. At the nano-scale, ordinary substances exhibit extraordinary behaviour's enhanced strength, novel optical effects, and unprecedented catalytic efficiency tailored to meet humanity's most pressing challenges [5,6].From ultra-precise drug delivery systems that target diseased cells without harming healthy tissue to next-generation optoelectronic devices that push the boundaries of computing and energy efficiency, nanotechnology is reshaping industries and igniting global scientific fervour [7].As we harness nature's own blueprints—through green synthesis and biomimetic designs nanotechnology transcends laboratory curiosity, emerging as a cornerstone of sustainable advancement. The journey has just begun, and the possibilities are as vast as the atomic building blocks themselves [2,8].

Metal nanoparticles have important uses in various conditions as optoelectronics, catalysis, biomedicine, & industrial effluent treatment processes, among others, because of their unique features [9,10]. The research community is particularly interested in metal

nanoparticles among other nanoparticles because of their unique characteristics and dependable, quick production methods [11,12]."Green synthesis" is the term used to describe the production of clean and eco-friendly nanoparticles using bacteria, fungi, plants, actinomycetes, and other species and is based on the widely acknowledged "green chemistry" concept [13,14]. In order to achieve sustainable development, green nanotechnology opens the door for the production of green nanoproducts and their exploitation. Due to the growing need to provide a process that is safe for the environment, clean, nontoxic, biocompatible, and economical, green synthesis has drawn more attention than conventional synthetic approaches [15].

Sennosides, which are derived from the pod shells and leaves of many species of Cassia, like *Cassia angustifolia* (Tinney Valley senna)& *c.acutifolia* (Alexandrian senna), are produced by the medicinal plant senna.Senna leaves and pod shell are used as a safe and effective purgative that promotes the colon's peristaltic movement [16,17]. Additionally, S. enterica, E. coli, Bacillus sp., S. aureus, and other microbes are inhibited in their growth by C. angustifolia and its mediated nanoparticles, such as ZnO, Ag, and TiO. Antibiotics and antifungal medications are typically used to treat bacterial and fungal illnesses. However, overuse of antibiotics kills the microbiota and causes the bacteria to become resistant, which results in a number of smaller issues [18]. As a result, certain alternative therapeutic approaches must be developed. Glycosides like the anthraquinone Sennosides are among the physiologically active components of C. angustifolia that are thought to be responsible for its antibacterial qualities [19,20].

2. Materials and Methods

2.1. Chemicals

We purchased fresh C. angustifolia leaves from the Alwar, Rajasthan, India, local market. I bought 99.8% pure copper sulfate and exceptionally pure sodium carbonate from SRL Chemicals in India. Sodium phosphate dibasic (0.5 M) and sodium phosphate monobasic (0.5 M) were used to create phosphate buffer (pH, 6.6). Gram-positive (S. aureus) and gram-negative (E. coli and P. aeruginosa) bacterial cultures were obtained from the nearby laboratory in the Alwar area of India. The solution used in the studies was made with distilled water. Every assay was carried out three times.

2.2. Green Synthesis of CuO nanoparticles using *Cassia angustiolia* extract

Using an alcoholic extract of Cassia leaves, CuO nanoparticles were made biologically. In order to create CuO nanoparticles, 90 mL of copper sulphate solutions and 10 mL of plant extract were well combined, and left to rest at room temperature after that [21]. The combination was incubated for four days, and both visual inspection & UV-vis spectroscopic measurements were used to track for development of NPs at regular intervals. The mixture was centrifuged for 15 minutes at 5000 rpm following incubation. The obtained pellet was centrifuged once more after being resuspended in a tiny amount of distilled water. To get rid of the contaminants, this procedure was carried out two or three times. The final pellet was dried in a hot air oven to eliminate any remaining moisture. After being dried, the particles were gathered and characterized [13,14].

2.3.Optimization of Drug Loaded Nanoparticles

To systematically analyse and optimize formulation parameters, the Box-Behnken Design (BBD-RSM) response surface methodology was utilized. The primary variables that determine the particle size andZeta potential of the CuO-NPs loaded with *C.angustifolia* extract production include formulation variables including homogenization speed and reaction temperature.

Table 1: Selection of variables or factors for the optimization of the CuO-NPs

Variable	**Symbol**	**Units**	**Levels**		
			-1	0	1
Critical Process Parameters or Independent factors for CS-MTX-SLNs					
Reaction temperature (°C)	X_1	°C	40	60	80
Speed of homogenization	X_2	rpm	5000	7500	10,000

2.4.Statistical analysis

Each group's results were presented as Mean ± SD, and one-way analysis of variance (ANOVA) and the Duncan's test for multiple comparisons were used to identify statistically significant differences between mean values. After statistical analysis, the data were deemed significant if $p < 0.05$.

3. Results

3.1.Optimization of Formulation variables of CuO Nano-Particles

Reaction temperature (X1) and homonization speed (X2), which varied across three levels (low (−1), medium (0), and high (+1)), were the two main parameters that were optimized. Zeta potential (Y2) (-mV) and particle size (Y1) (nm) measurements were used to characterize the resultant CuO-NPs. The answers in the CCD model were these measurements (Table 2). The range for Nanoparticles particle size is 100.8 to 130.5 nm, and for ZP in the range of -21.8 to -34.2.Suitable model for particle sizewas linear modelas no effect of interactions between the factors were observed on this attribute &for ZP quadratic modelas interactions between the factors were found to affect these attributes in both responses.

The data modeling technique yielded polynomial equations (1) and (2), which showed that the examined response variables, particle size, and zeta potential, had both interaction and curvature effects.

Y1 (Particle Size) = + 114.44-7.75A-1.45B……Eqs.1

Y2 (Zeta Potential) = -22.23 + 1.69A + 2.84B - 0.8750AB – 3.45 A^2 – 1.95B^2……Eqs.2

Table 2: Design matrices for experiments to optimize CuO-nanoparticles made from leaf extract from C. angustifolia

Std	**Run**	**F 1**	**F 2**	**R 1**	**R 2**
		Reaction Temp (°C)	**Sonication (rpm)**	**Particle Size (nm)**	**Zeta Potential (mV)**
5	1	31.7157	7500	117.5	-30.8

13	2	60	7500	110.2	-21.89
6	3	88.2843	7500	100.8	-26.7
9	4	60	7500	119.6	-22.54
7	5	60	3964.47	111.8	-29
3	6	40	10000	118.7	-25.7
2	7	80	5000	108	-28.6
1	8	40	5000	130.5	-34.2
4	9	80	10000	102.8	-23.6
11	10	60	7500	118.7	-22.15
8	11	60	11035.5	115.6	-22.5
10	12	60	7500	110.7	-22.78
12	13	60	7500	122.8	-21.8

A strong connection between the experimental and projected responses was shown by the model summary statistics, which showed R^2 values of 0.6195 for Y1 (particle size), and 0.9759 for Y2 (Zeta Potential) for the two response models.Furthermore, a relatively good agreement was seen between the adjusted R^2 value (0.5433 for Y1, and 0.9586 for Y2) and the anticipated R^2 value (0.3487 for Y1, and 0.8485 for Y2), suggesting the dependability of the models.For the responses Y1 and Y2 the factor effects and corresponding p-values are shown in Tables 6.6 and 6.7 Each coefficient's significance was assessed using the p-value (<0.0001). The corresponding coefficient is more significant the smaller the p-value.

Effect of Formulation parameters on Particle Size (Y1)

Three-dimensional response surface plots and two-dimensional contour plots were employed to visualize and analyse the interactions between independent variables and their influence on the response variables.

Table 3:ANOVA for the particle size response linear model (Y1)

Source	**Sum of Squares**	**df**	**Mean Square**	**F-value**	**p-value**	
Model	497.66	2	248.83	8.14	0.0080	significant
A-Reaction Temp	480.77	1	480.77	15.73	0.0027	
B-Sonication Speed	16.90	1	16.90	0.5526	0.4743	
Residual	305.73	10	30.57			
Lack of Fit	178.31	6	29.72	0.9329	0.5536	not significant
Pure Error	127.42	4	31.85			
Cor Total	803.39	12				

Std. Dev.	5.53	**R^2**	0.6195
Mean	114.44	**Adjusted R^2**	0.5433
C.V. %	4.83	**Predicted R^2**	0.3487
PRESS	523.24	**Adeq Precision**	8.2549

Response surface analysis revealed a strong inverse correlation between temperature/sonication speed and particle size, with higher values of both parameters yielding smaller particles. Zeta potential, however, exhibited a nonlinear relationship, dipping to its lowest levels only at the upper and lower bounds of the tested temperature and speed ranges.

It was clear that at lower temperature, the particle size decreases from 130.5 nm to 118.7 nm when the sonication speed increases from low level to high level.It was clear that at low level of sonication speed, the particle size decreases from 130.5 nm to 108 nm when the reaction temperature increases from low level to high level. Minimum particle size 102.8 was observed when both the reaction temp 80^0C and speed 10000rpm was highest.

Effect of Formulation parameters on Zeta Potential (Y2)

The contour and 3D plots demonstrate the linear effect of the independent components on Zeta Potential, as indicated by the equation's lack of evidence of factor interactions. However, only the Sonication Speed (X2) had a significant ($p < 0.0001$) impact on the Zeta Potential for CuO-NPs, as shown by the ANOVA results (Table 4). With a difference of less than 0.2, the Predicted R2 of 0.8485 and the Adjusted R2 of 0.9586 are in reasonable agreement.

Table 4:ANOVA for response linear model for Zeta Potential (Y2)

Source	**Sum of Squares**	**df**	**Mean Square**	**F-value**	**p-value**	
Model	189.11	5	37.82	56.59	< 0.0001	significant
A- Temp	22.78	1	22.78	34.08	0.0006	
B-Sonication Speed	64.37	1	64.37	96.31	< 0.0001	
AB	3.06	1	3.06	4.58	0.0696	
A^2	82.93	1	82.93	124.09	< 0.0001	
B^2	26.53	1	26.53	39.69	0.0004	
Residual	4.68	7	0.6683			
Lack of Fit	3.97	3	1.32	7.51	0.0404	significant
Pure Error	0.7055	4	0.1764			
Cor Total	193.79	12				
Mean	-25.56	**Adjusted R^2**			**0.9586**	
C.V. %	3.20	**Predicted R^2**			**0.8485**	
PRESS	29.35	**Adeq Precision**			**19.64**	

It was demonstrated that when the temperature of reaction (X_1) rose from 40-80°C, the ZP increased from -34.2 to -28.6 at a lower degree of speed 5000rpm (X_2). In a similar manner, when speed (X_2) went from low to high level at a high degree of temp (X_1), the ZP increased from -29 (mV) to -22.5(mV). The findings showed that a high temperatureand high speed raises the drug's Zeta Potential, which may be because the medication penetrates the medium more readily when temperatureis high. Graphs dem on strated that an enhanced in speed from low to medium degree led to an increase in ZP from -30.8 to -26.7 at highest degree of temperature.

These statistics show that when the temp goes fromlower to a higherdegree 40-80^{0}C, the ZP increases from -25.7 to -23.6 at a highest level of speed. Similar to this, when speed increases from low to high level, the ZP increased from -34.2 to 22.54 at lower level of temp (X2).

Data optimization and validation of experimental model

After ANOVA, the Design-Expert® program was used to provide appropriate solutions for each response's required quality attributes of Cu)-NPs in order to produce an optimum formulation. The replies' design space (overlay plot) was created (Fig. 1, 2), and the solution (Table 5, 6) that had a desirability of 0.55 and fell inside the overlay plot's shaded (yellow) region was selected (Fig. 1, 2).The solution's X1 = 114.187 and X2 = -21.8, variables, in turn, correlated with the 60^{0}C of temp and 7932.117 rpm homogenization speed, respectively. The trials were run in triplicate using the selected solution, and the results were noted. Following the checkpoint analysis, it was discovered that the outcomes agreed with the anticipated values.

To validate the efficacy of the optimization process, a fresh batch of CuO-NPs was created with the anticipated formulation factor levels. The pre-selected target response goals in the Design-Expert optimization algorithm employing the desirability function were set to "maximize." Concurrently, the particle size value of "important" was set to minimize and the Zeta potential value was set to in range.

Table 5: The Numerical Optimization Criteria-CuO-NPs

Characteristics	**Goal**	**Lower Limit**	**Upper Limit**	**Lower Weight**	**Upper Weight**	**Importance**
A: Reaction temperature	is equal to 60	40	80	1	1	3
B: Sonication Speed	is in range	5000	10000	1	1	3
Particle size	minimize	100.8	130.5	1	1	3
Zeta potential	is in range	-34.2	-21.8	1	1	3

Reaction Temperature	**Sonication Speed**	**Particle size**	**Zeta potential**	**Desirability**
60	7932.177	114.187	-21.800	0.549

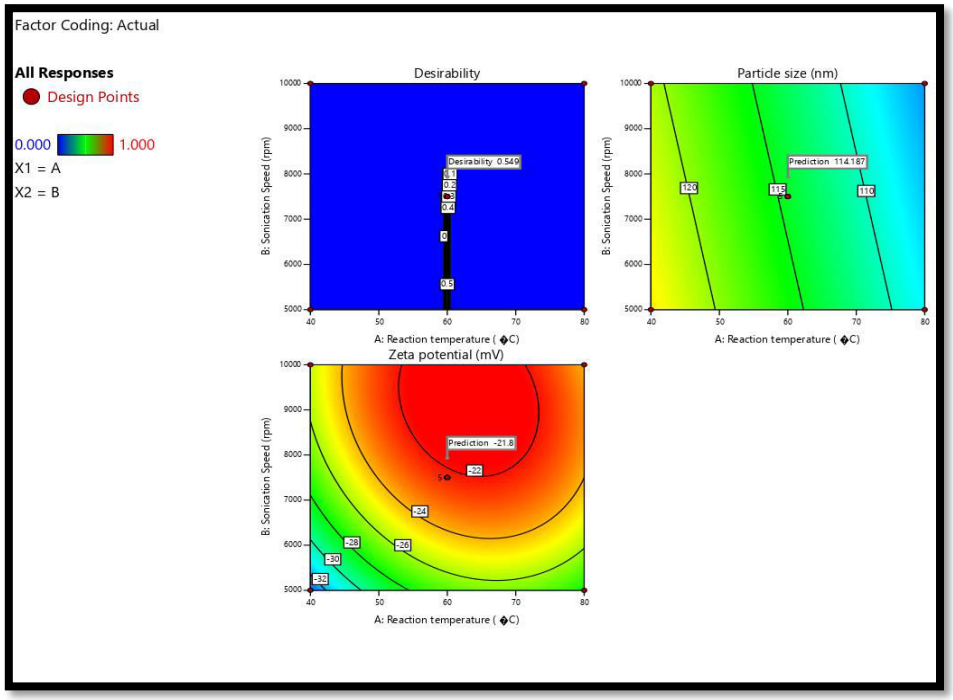

Figure 1: Desirability plot showing the design space for the responses for CuO-NPs

Table6: Comparison of the anticipated reaction and the experimentally observed responses of the optimized CuO-NPs formulas

Process	**X_1 °C**	**X_2 rpm**	**Predicted**	**Experimental (n=3)**	**Error(%)**
Particle size (Y1)	60	7932	114.18	111.65 ± 1.79	2.2
ZP (Y2)	60	7932	-21.8	-22.6 ±0 .054	3.66

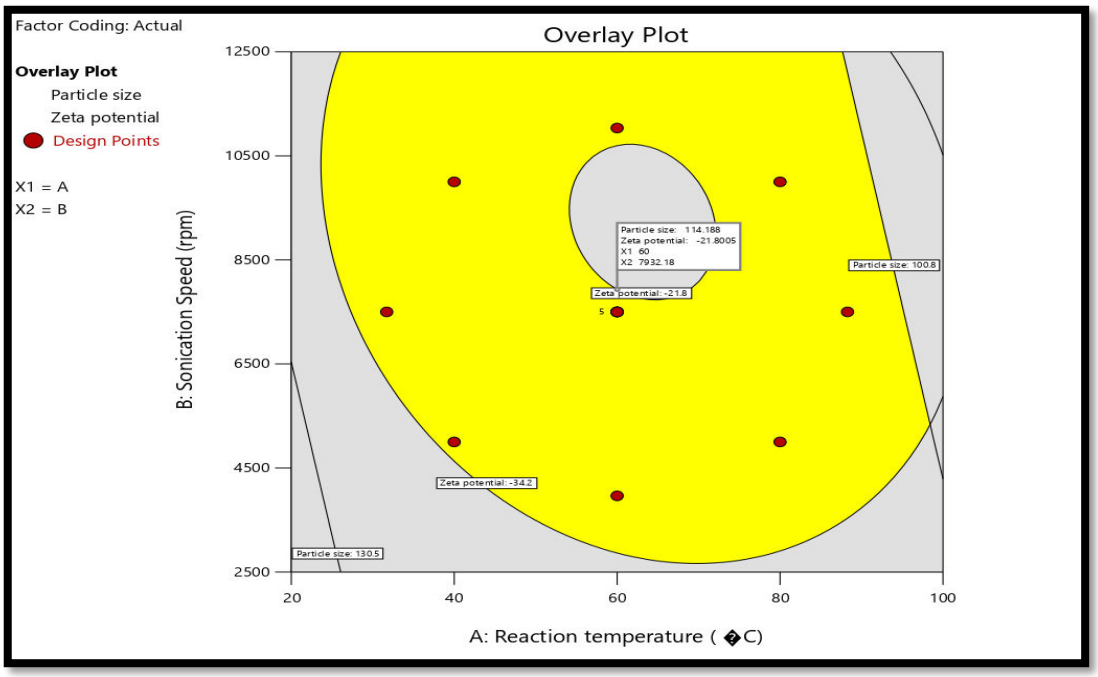

Figure2: Overlay plot showing the design space for the responses generated by the Design-Expert® software for CuO-NPs.

The improved formulation showed good agreement with the expected values, having particle size 111.65±1.79 nm and ZP -22.6 ±0 .054. The values of the observed reactions & those predicted by mathematical models are displayed in Table 6, together with the prediction error percentage. The response parameters had prediction errors of 2.2 and 3.66%, with an absolute error value of 2.94 ± 0.1%. These results also show that the constructed models are suitable and that the results of the predictions accord well with the measured data.

Characterization of Optimized batch ofCuO NPs

Optical Characterization (Ultra violet and visible spectrometric analysis)

The synthesized sample was exposed to UV-vis to verify creation of CuO nanoparticles, and the resulting spectra are shown in Figure 3.The mixture's colour change served as a visual indicator of the C. angustifolia extract's conversion of Cu^{2+} ions to CuO NPs. After 4 days, the solution's colour gradually altered from pale green to dark brown, indicating that phytochemicals and phenolic compounds in the extract of C. angustifolia serve as an effective reducing agent for the synthesis of CuO-NPs [22].

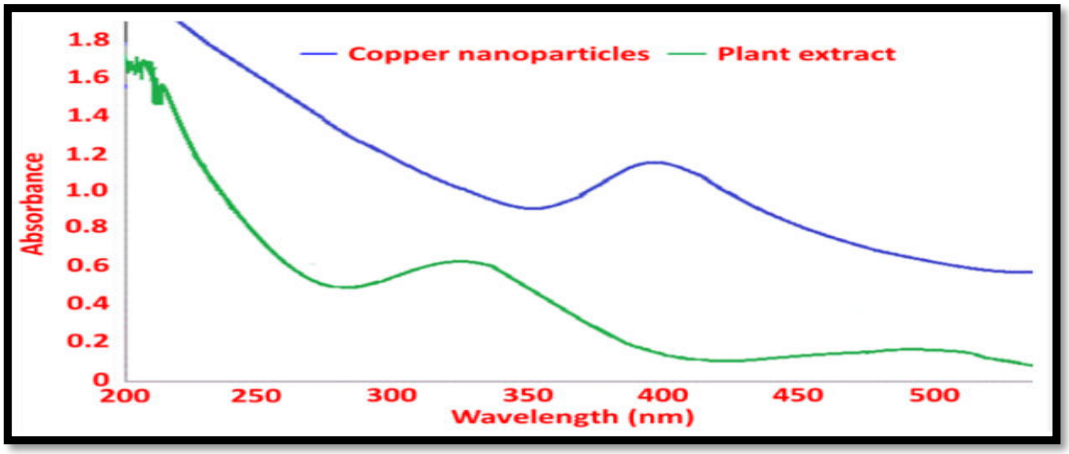

Figure 3:UV–Vis spectra of CuO NPs using *C. angustifolia* leaf extract

The creation of the desired CuO nanoparticles is confirmed by the observation that the highest absorbance of ordinary leaf extract occurs between 300 and 350 nm, while for CuO nanoparticles, it occurs between 350 and 400 nm.The absorption peak of bulk CuO is red-shifted at higher wavelengths, but as particle size decreases, the peak's position becomes blue-shifted (towards a lower wavelength) The absorption peak of CuO in this work, however, occurs at a significantly lower wavelength (blue-shifted) at about 400 nm, which is where smaller CuO NPs are expected to develop.

FT-IR spectrum analysis

The C-H functional group of alkanes is represented by the peaks 2919.1 cm^{-1}& 2849.97 cm^{-1}. The N-H bend of amide groups, which is a feature of the proteins found in the C. angustifolia leaves, was visible in the peaks seen at 1638.6 cm-1 and 1606 cm-1. It is possible to attribute the peak 1384.44 cm-1 to aromatics C–C Stretch (In–Ring)(Table 7).

Table 7: Interpretation of FT-IR Spectrum of CuO-NPs

Stretching type	**Spectra Range Standardcm^{-1}**	**Observedpeakcm^{-1} CuO-NPs**
O-HStretching (Phenol)	3700-3200	3413
C-Hbending	3000-2850	2919, 2849
N-Hbending	1780-1570	1638, 1606
C–C Stretch (In–Ring)	1520-1350	1384
C-O-Cstretching	1210-1040	1072
Cu-O vibrations	850-600	625

Particle size and Zeta potential analysis

The size and ZP of particles in a solution or suspension, usually in the submicron range, can be ascertained using the Dynamic Light Scattering (DLS) technique. According to DLS analysis, the produced CuO-NPs showed a very consistent size distribution with a hydrodynamic diameter of 111.65 nm and a zeta potential of -22.6 mV (Fig. 4).

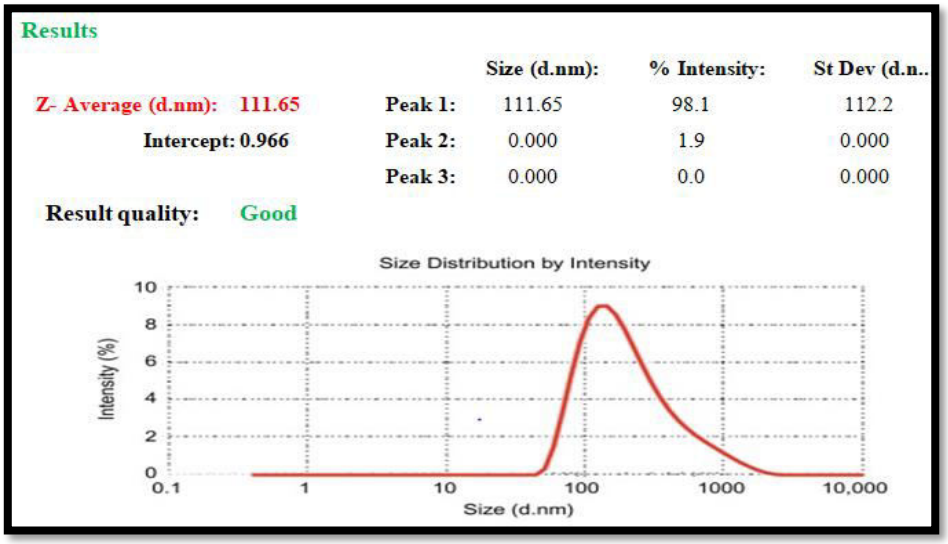

Figure 4: Particle size distribution of optimized batch of CuO-NPs

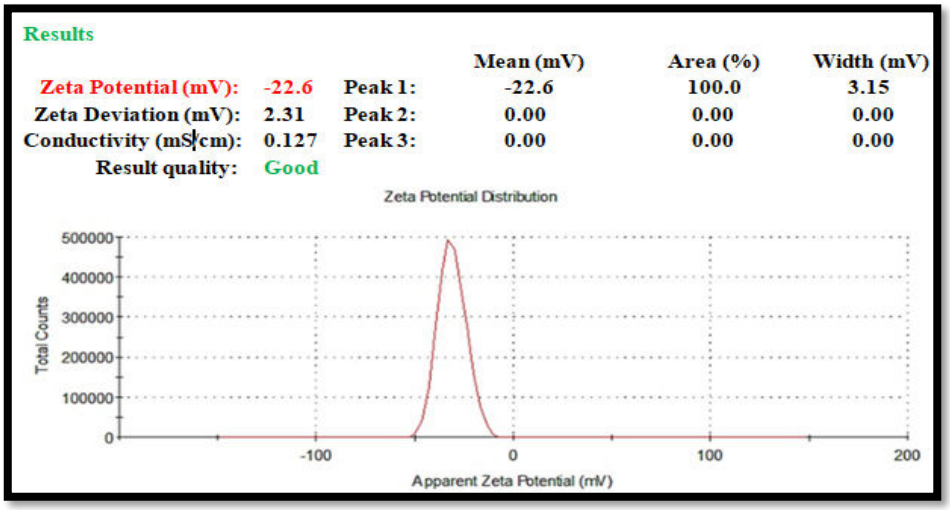

Figure 5: Zeta potential of optimized batch of CuO-NPs

Generally, stable nanoparticle dispersions need a zeta potential greater than ±30 mV. Because of the capping effect of the bioorganic compounds in the plant extract, the

produced CuO-NPs showed a negative zeta potential (Fig. 5). Strong electrostatic repulsion between particles is encouraged by this negative charge, which keeps particles from clumping together and guarantees colloidal stability.

Transmission Electron Microscopy (TEM) Analysis of CuO nanoparticles

TEM analysis utilizes to study the precise shape & structure of the CuO nanoparticles made from C. angustifolia extract. The existence of spherical particles with sizes ranging from 20 nm to 30 nm is evident from TEM pictures (Fig.6). The crystalline character of the plant extract-mediated produced CuO-NPs was further demonstrated by TEM studies.

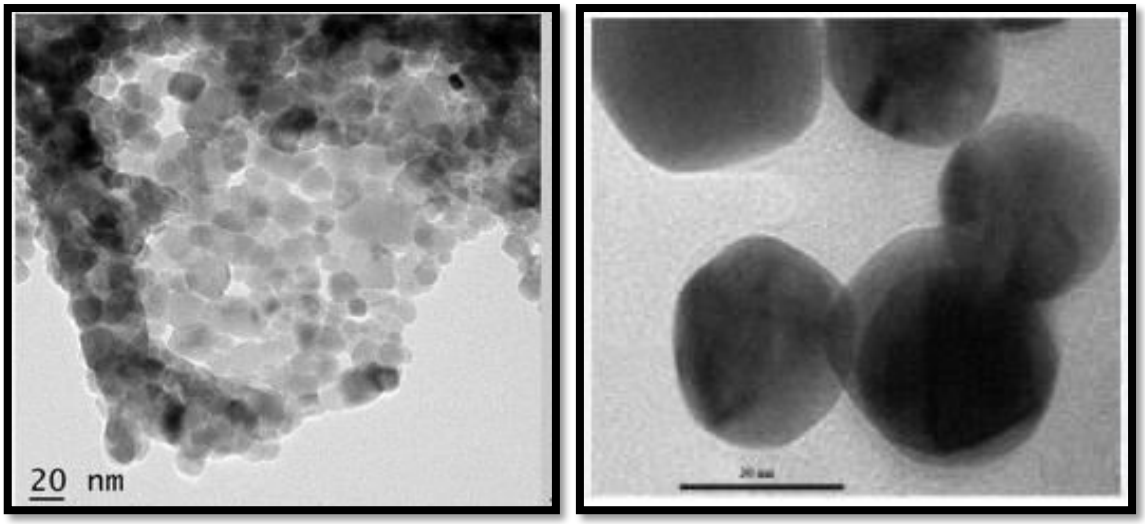

Figure 6:TEM analysis of CuO nanoparticles and SAED pattern

XRD analysis of CuO nanoparticles

Fig. 7 displays the formulation's X-ray diffraction pattern from the leaf extract. The nanoparticles' X-ray diffraction (XRD) pattern as determined by colloid samples, further demonstrated the formulation's crystalline structure. X-ray diffraction analysis of the formulation verified that the particles were crystalline. For the (111), (202), (220), (202), (113), (022), and (113), several Bragg reflections with 2ø values of 38.12°, 47.52°, 54.38°, 58.92° and 61.42°, 67.52°, 69.25° correspond to metallic reflections When compared to normal powder diffraction, Cu clearly shows the cubic crystalline face-centered cubic structure of copper.

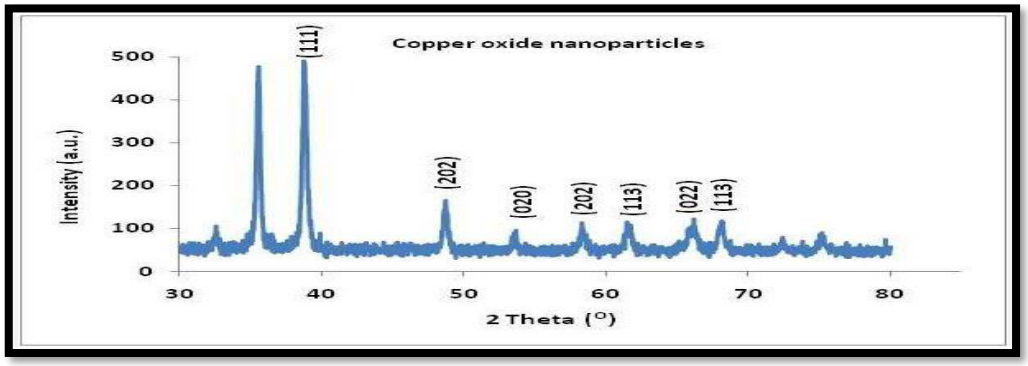

Figure 7:XRD pattern of CuO nanoparticles synthesized by C. angustifolia

SEM analysis of CuO nanoparticles

SEM studyshows that the nanoparticles were spherical and crystalline, with sizes ranging from 20.25 to 62.5 nm (Fig.8). When observed under a SEM, the majority of the NPs collected and only a small portion were dispersed. The nanoparticles' average size is determined to be between 30 and 40 nm, which closely match the results of the XRD and TEM analyses.

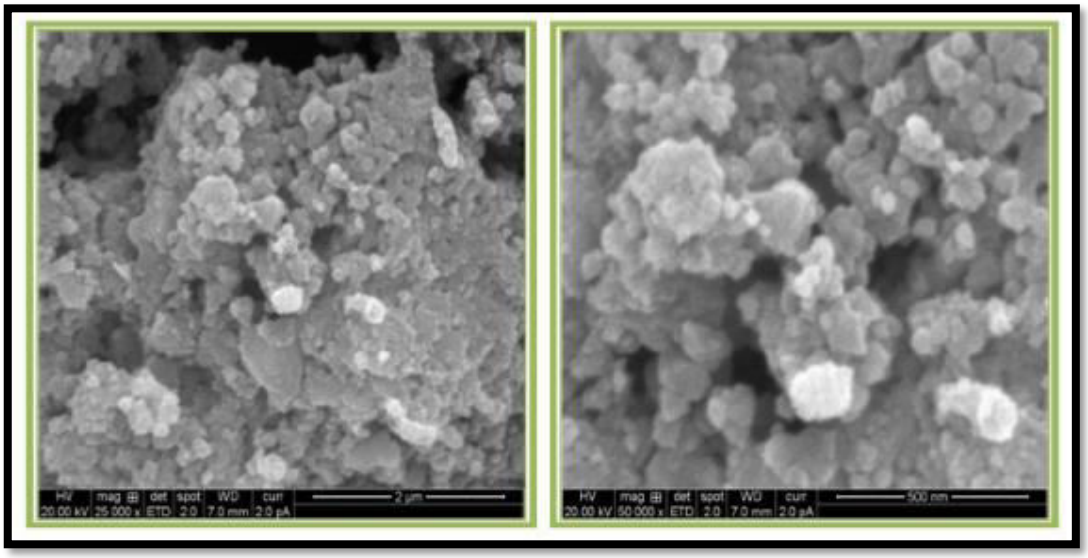

Figure 8: SEM Analysis ofCuO nanoparticles under different magnifications

Energy Dispersive X-ray Analysis (EDX) analysis of CuO-NPs

The chemical identification of the produced particles is determined by EDX analysis. The EDX spectrum (Fig. 9), which also confirms XRD data, shows the presence of Cu at 0.8 to 1.2 keV and oxygen atoms at 0.5 keV without any other material. The findings showed that the nanoparticles were made of CuO nanoparticles with a high degree of purity. The observed atomic percent values were 28.88 for oxygen and 71.12 for copper with CuO.

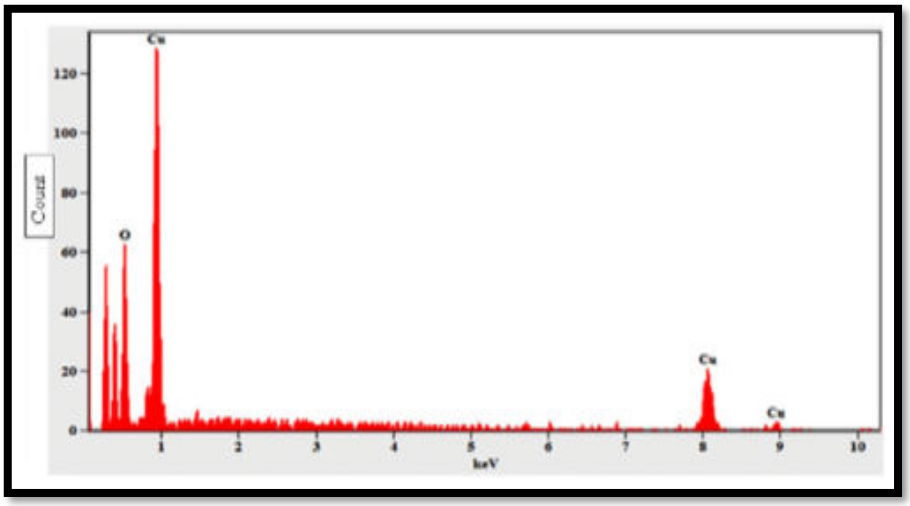

Figure 9:EDS-Spectroscopy of the C. angustifolia showing synthesis of CuO nanoparticles and elemental Cu signal in higher percentage

Conclusion

An economical and environmentally favourable substitute for traditional chemical and physical processes is the green synthesis of copper oxide nanoparticles, which can be accomplished with plant extracts, microbes, or other environmentally benign reducing

agents. This method reduces the usage of dangerous chemicals, reduces energy consumption, and aligns with the principles of green chemistry. Optimization of synthesis parameters through response surface methodology (RSM) such as temperature, and reaction speed—plays a crucial role in controlling the size, morphology, and stability of the nanoparticles. Advanced characterization techniques—including UV-Vis spectroscopy, XRD, FTIR, SEM, and TEM—collectively confirmed the successful synthesis and structural properties of the CuO nanoparticles (NPs) with desired properties for various applications, including catalysis, antimicrobial activity, sensing, and energy storage. Future research should focus on scaling up production, improving reproducibility, and exploring novel biological sources for synthesis. Additionally, in-depth studies on the mechanism of nanoparticle formation and their long-term stability will facilitate broader industrial and biomedical applications. Overall, green-synthesized CuO NPs hold great promise for sustainable nanotechnology development.

Conflicts of Interest: Regarding the publishing of this work, the authors state that they have no conflicts of interest.

References:

1. Malik S., Muhammad K., and Waheed Y. (2023). Nanotechnology: A Revolution in Modern Industry. Molecules (Basel, Switzerland), 28(2), 661.
2. Singh J., Dutta T., Kim K. H., Rawat M., Samddar P., and Kumar P. (2018). 'Green' synthesis of metals and their oxide nanoparticles: applications for environmental remediation. Journal of nanobiotechnology, 16(1), 84.
3. MishraRK. and Agarwal R. (2024) Research and reviews in nanotechnology. Published by Bhumi publishing; Volume I: 115-132
4. Nalwa H.S.(1999)Handbook of Nanostructured Materials and Nanotechnology, Five-Volume Set; Academic Press: Cambridge, MA, USA, ISBN 9780080533643.
5. Thiruvengadam M., Chung I. M., Gomathi T., Ansari M. A., Gopiesh Khanna V., Babu V., and Rajakumar G. (2019) Synthesis, characterization and pharmacological potential of green synthesized copper nanoparticles. Bioprocess and biosystems engineering, 42(11), 1769–1777.
6. Bhavyasree P. and Xavier T. (2021)Green synthesised copper and copper oxide based nanomaterials using plant extracts and their application in antimicrobial activity: Review. Curr. Res. Green Sustain. Chem., 5, 100249.
7. Kumar RS., Menon S.,and Venkat Kumar S. (2021) Anti-Inflammatory and Antimicrobial Potential of Cassia -Assisted Copper Oxide Nanoparticles. J. Nanomater: 1–11
8. Iravani S. (2011) Green synthesis of metal nanoparticles using plants. Green Chem., 13(10), 2638–2650.
9. Amjad R., Mubeen B., Ali S.S., Imam S.S., Alshehri S., and Ghoneim M.M. (2021) Green Synthesis and Characterization of Copper Nanoparticles Using Fortunellamargarita Leaves. Polymers, 13, 4364.
10. Cheirmadurai K., Biswas S., Murali R.and Thanikaivelan P. (2014) RSC Advances, vol.4, no.37, pp.19507-19511.

11. Sukumar S.,Rudrasenan A.,and Nambiar D.P. (2020)Green-Synthesized Rice-Shaped Copper Oxide Nanoparticles Using Caesalpinia bonducella Seed Extract and Their Applications. ACS Omega, 5, 1040–1051.
12. Sutradhar P., Saha M.,and MaitiD. (2014)Microwave synthesis of copper oxide nanoparticles using tea leaf and coffee powder and its antibacterial activity", Journal of Nanostructure in Chemistry, vol.4, pp.86
13. Almisbah SRE., and Mohammed AMA.(2023) Green synthesis of CuO nanoparticles using Hibiscus sabdariffa L. extract to treat wastewater in Soba Sewage Treatment Plant, Sudan. Water Sci Technol; 87(12):3059-3071.
14. İnce S., Yalçın MS., İnce T., and Geçgel C. (2023) Green Synthesis of CuO Nanoparticles Using Agaricus bisporus Extract as a Highly Efficient Catalyst for the Suzuki Cross-Coupling Reaction. Chem Biodivers ;20(12): e202301411.
15. Mallakpour S.,& Madani M. (2015)A review of current coupling agents for modification of metal oxide nanoparticles, Progress in Organic Coatings, vol. 86, pp.197-207.
16. Kokate C. K., Purohit A.P., and Gokhale S.B.(2003) Ed. Pharmacognosy, 25thEdn, Nirali prakashan: 77-85
17. Singanaboina K.,and Chinna V. (2018) Pharmacognosy of Cassia angustifolia Leaf Grown in Differently Treated Soils. International Journal of Current Microbiology and Applied Sciences. Special Issue-6: 2580-2589
18. Uddin M.T., Chakraborty A.J, and Khusro A. (2021) Antibiotic resistance in microbes: History, mechanisms, therapeutic strategies and future prospects. Journal of Infection and Public Health. 14 (12): 1750-1766
19. Huq M.A., Apu M.A.I., and Ashrafudoulla M. (2023) Bioactive ZnO Nanoparticles: Biosynthesis, Characterization and Potential Antimicrobial Applications. Pharmaceutics. 16;15(11):2634. doi: 10.3390/pharmaceutics15112634.
20. Peng F., Sun Y., Lu Y., Yu W., Ge M., Shi J., Cong. R., Ha J., and Dai N(2020) Studies on Sensing Properties and Mechanism of CuO Nanoparticles to H2S Gas. Nanomaterials, 10, 774
21. Das P.E., Abu-yousef I.A.,and Majdalawieh A.F. (2020) Narasimhan, S. Green Synthesis of Encapsulated Copper Nanoparticles Using a Hydroalcoholic Extract of Moringa oleifera Leaves and Assessment of Their Anti-oxidant and Anti-Microbial Activities Supplementary Figure 1. Resazurin Microtiter Assay Pla. Molecule, 25, 555
22. Rajendran S.P., and Sengodan K. (2017) Synthesis and Characterization of Zinc Oxide and Iron Oxide Nanoparticles Using Sesbania grandiflora Leaf Extract as Reducing Agent. J. Nanosci., 2017, 1–7.